Exploring the association of Fermi sources with Young Stellar Objects

P. Munar-Adrover[1], J.M. Paredes[1], G.E. Romero[2]

UNIVERSITAT DE BARCELONA

ICCUB

[1] Departament d'Astronomia i Meteorologia and ICCUB, Universitat de Barcelona (IEEC-UB)
[2] Instituto Argentino de Radioastronomía (CCT La Plata, CONICET)

I A R
CCT La Plata
CONICET

Abstract

Massive protostars have associated bipolar outflows which can produce strong shocks when interact with the surrounding medium. In these conditions particle acceleration at relativistic velocities can occur leading to gamma ray emission, as some theoretical models predict. To identify young stellar objects (YSO) that may emit gamma rays we have crossed the Fermi First Year Catalog with some catalogs of known YSOs, and we have conducted Montecarlo simulations to find the probability of chance coincidence. With this crossing we obtained a list of YSOs spatially coincident with Fermi sources that may show gamma ray emission. Our results indicate that ~70% of the candidates should be γ-ray sources with a confidence of ~5σ. We have studied the coincidences one by one to check the viability of these YSOs as potential counterparts of Fermi sources and plan further detailed observations of few of them.

γ-ray production scenario

Massive YSOs show collimated outflows and thermal radiation has been detected up to distances of 10^{16}-10^{18}cm from the central star. These are strongly supersonic jets and in some cases, non-thermal radio lobes have been detected at distances of Z_j~ 1pc (Garay et al. 2003). These radio lobes are probably generated by strong terminal shocks of the jets, which also ionize the shocked material. The possibility of YSOs to be γ-ray emitters has already been discussed in Araudo et al. 2007 and Bosch-Ramon et al. 2010.

Magnetic fields should also be present, since they play an important role in supporting the cloud before the gravitational collapse. Under these conditions, particles can be accelerated up to relativistic energies via diffusive shock (Fermi I) acceleration (e.g. Bell 1978). These particles would produce the non-thermal radiation found in the lobes and could generate significant emission in a broad spectral range, from radio to γ-rays (Bosch-Ramon et al. 2010). We assume, that the non-thermal radio lobes are the regions in which protostellar jets terminate.

The action of the jet head on the external medium leads two shocks (Fig. 1), one moving in the cloud material and one moving in the jet itself: the bow shock and the reverse shock, respectively. The observed non-thermal radio emission would be generated at the shocks where the particles are accelerated.

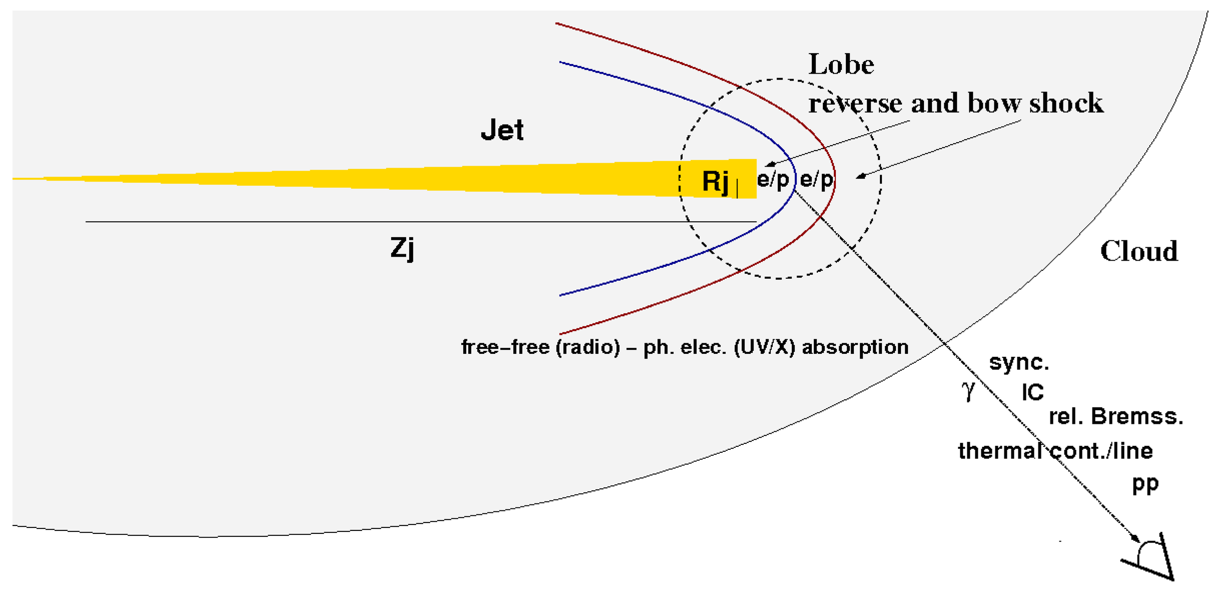

Fig. 1. Diagram of the termination region of the jet of a massive YSO. The two shocks are represented. Particles can be accelerated in these shocks and produce non-thermal radiation via interaction with the surrounding matter, the radiation field and the magnietic field. (Bosch-Ramon et al. 2010)

The First Fermi-LAT Catalog (1FGL)

The 1FGL contains 1451 high-energy sources detected in the 100 MeV to 100 GeV range by the Large Area Telescope, the primary science instrument on the Fermi Gamma-ray Space Telescope during the 11 months of the science phase of the mission, which began on 2008 August 4 (Abdo et al. 2010). The 1FGL includes source location regions, defined in terms of elliptical fits to the 95% confidence regions, power-law spectral fits and flux measurements in 5 energy bands for each source.

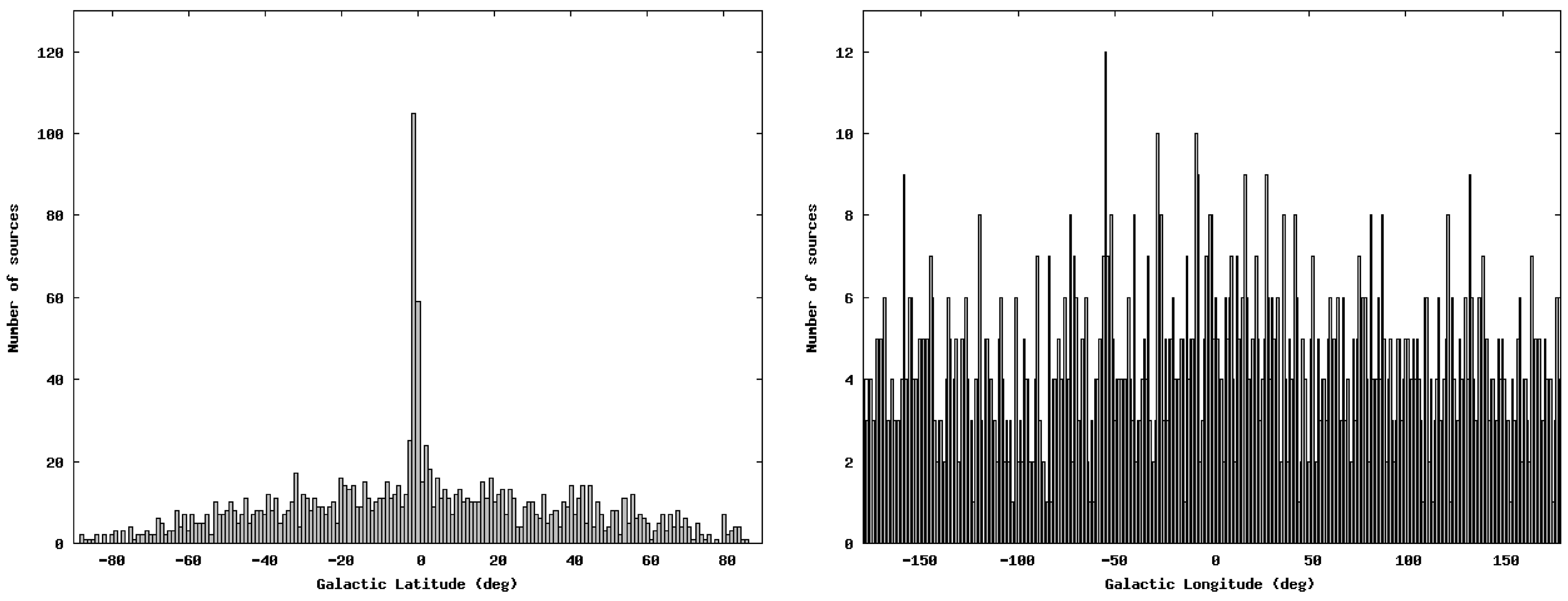

Fig. 2. 1º-binning distribution in galactic latitude (left) and longitude (right) of the 1392 Fermi sources used in the simulations.

The RMS Survey

MYSOs are luminous (L > $10^4 L_{Sun}$), embedded infrared sources that still have to begin to ionize their surroundings to form an ultra-compact H II region. They are likely to be already burning hydrogen in their cores, whilst still accreting at the surface. They drive bipolar molecular outflows and often have a compact ionized stellar wind and associated maser activity. Most of their energy comes out in the infrared after reprocessing by the dense circumstellar dust envelope. This is therefore the most logical and unbiased way of searching for such objects.

The Red MSX Source (RMS) survey is an ongoing multi-wavelength observational program with the objective of providing a well-selected sample of MYSOs in the entire Galaxy (Urquhart et al. 2009). They have identified ~2000 MYSO candidates by comparing the colours of MSX and 2MASS point sources with those of well known MYSOs.

The survey also uses high resolution radio continuum observations at 6cm obtained with the VLA in the northern hemisphere, and at 3.6 cm and 6 cm with ATCA in the southern hemisphere, that help to distinguish between genuine MYSOs and other types of objects, such as Ultra Compact HII regions, evolved stars or Planetary Nebulae, that contaminate the sample.

In addition to these targeted observations, archival data of previous VLA survey of the inner Galaxy has been used.

This ongoing program has provided a sample of 556 well identified MYSOs up to day, which have been used in our work.

Method

- We have used a computer code that determines the angular distance between two points in the sky, taking into account the positional uncertainties in each of them.
- We ran the code with the 1392 sources of the 1FGL that have not been firmly identified, and the 556 sources identified as YSOs in the RMS survey (J.S. Urquhart et al. 2009).
- We have found 13 γ-ray sources of the 1FGL catalog positionally coincident with YSOs from the RMS Survey. In order to estimate the statistical significance of these coincidences, we have simulated a large number of sets of Fermi sources. Specifically, we have simulated 1500 populations of 1392 Fermi sources, through rotations on the celestial sphere, displacing a source with original galactic coordinates (l, b) to a new position (l_0, b_0) (as in Romero et al. 1999).
- The new positions have been obtained by doing l_0 = l+R_1 x 360º, where R_1 is a random number between 0 and 1. In order to retain the histogram of the distribution of sources in galactic latitude (Fig. 2) we replace b_0 = b+R_2 x 1º, and then, if the integer part of b_0 is greater than the integer part of b or if the sign of b_0 and b are different, we replace b_0 by b_0 + 1º. Similarly, we have conducted a second simulation, using a 2º-binning distribution.
- The separation between the Fermi source and the YSO is calculated in each case using the statistical parameter R (Allington-Smith et al. 1982)

$$R=\sqrt{\frac{(\Delta\alpha\cos\delta)^2}{\sigma_{i_\alpha}^2+\sigma_{j_\alpha}^2}+\frac{\Delta\delta^2}{\sigma_{i_\delta}^2+\sigma_{j_\delta}^2}}\leq 1$$

where $\sigma_{\alpha i}$, $\sigma_{\delta i}$ is the uncertainty in the position of the source, and *i* and *j* are Fermi and RMS sources, respectively. The case R=1 means that the RMS source is just on the border of the error ellipse of the Fermi source.

Fermi Name	RA °	Dec °	95% Semi Major Axis °	Spectral Index Γ ($F \propto E^{-\Gamma}$)	Energy Flux erg cm^{-2} s^{-1}	MSX Name	RA hh:mm:ss	Dec ° :′:″	Freq. GHz	Int.Flux mJy	Angular dist. °	R
1FGL J0541.1+3542c	85.2805	35.7091	0.1397	2.41±0.13	$1.61\times10^{-11}\pm4.9\times10^{-12}$	G173.6328+02.8064	05:41:07.12	+35:49:37.2	5	< 0.7	0.12	0.846
						G173.6339+02.8218	05:41:11.18	+35:50:03.4	5	< 0.7	0.13	0.903
						G173.6882+02.7222	05:40:54.62	+35:44:08.1	5	< 0.8	0.05	0.364
						G173.7215+02.6924	05:40:52.32	+35:41:29.7	5	< 0.8	0.05	0.386
1FGL J0647.3+0031	101.8417	0.5289	0.2150	2.41±0.11	$1.89\times10^{-11}\pm5.4\times10^{-12}$	G212.0641−00.7395	06:47:13.31	+00:26:06.0	5	< 0.9	0.10	0.467
1FGL J1256.9−6337c	194.2474	-63.6212	0.1955	2.26±0.12	$4.97\times10^{-11}\pm1.1\times10^{-11}$	G303.5990−00.6524	12:57:25.31	−63:30:59.4	4.8	< 0.6	0.12	0.589
1FGL J1315.0−6235c	198.7635	-62.5971	0.1860	2.31±0.12	$6.86\times10^{-11}\pm0.0$	G305.4840+00.2248	13:13:36.04	−62:32:13.5	8.6	< 2.1	0.18	0.958
						G305.5610+00.0124	13:14:25.82	−62:44:30.8	8.6	7.2	0.16	0.869
1FGL J1651.5−4602	252.8831	-46.0340	0.2258	2.21±0.07	$1.39\times10^{-10}\pm3.4\times10^{-11}$	G339.8838−01.2588	16:52:04.66	−46:08:33.6	8.6	2.6	0.14	0.638
1FGL J1702.4−4147c	255.6039	-41.7859	0.0800	2.39±0.07	$8.7\times10^{-11}\pm2.0\times10^{-11}$	G344.4257+00.0451B	17:02:08.82	−41:46:58.9	8.6	< 13.7	0.05	0.631
						G344.4257+00.0451C	17:02:08.61	−41:47:10.2	8.6	< 13.7	0.05	0.638
1FGL J1846.8−0233c	281.7001	-2.5628	0.1262	2.21±0.06	$9.3\times10^{-11}\pm2.3\times10^{-11}$	G030.1981−00.1691	18:47:03.06	−02:30:36.1	5	< 0.8	0.08	0.646
1FGL J1848.1−0145c	282.0470	-1.7605	0.0859	2.23±0.04	$9.5\times10^{-11}\pm3.2\times10^{-11}$	G030.9726−00.1410	18:48:22.03	−01:48:30.3	5	< 0.7	0.07	0.763
						G030.9959−00.0771	18:48:10.84	−01:45:29.1	5	< 1.2	0.00	0.036
1FGL J1853.1+0032c	283.2884	0.5366	0.5207	2.18±0.07	$5.7\times10^{-11}\pm1.7\times10^{-11}$	G032.8205−00.3300	18:52:24.60	−00:14:57.7	5	< 0.7	0.34	0.658
						G033.3891+00.1989	18:51:33.82	+00:29:51.0	5	< 1.0	0.40	0.768
						G033.3933+00.0100	18:52:14.66	+00:24:55.0	5	< 1.1	0.26	0.496
						G034.0126−00.2832	18:54:25.05	+00:49:56.6	5	< 0.7	0.43	0.830
						G034.0500−00.2977	18:54:32.29	+00:51:32.9	5	< 0.8	0.47	0.908
1FGL J1925.0+1720c	291.2748	17.3485	0.1443	2.28±0.12	$2.37\times10^{-11}\pm1.02\times10^{-11}$	G052.2078+00.6890	19:25:08.51	+17:24:48.2	5	< 0.7	0.08	0.533
						G052.2025+00.7217A	05:40:54.62	+35:44:08.1	5	< 0.8	0.07	0.453
1FGL J1943.4+2340c	295.8667	23.6815	0.1118	2.23±0.11	$2.62\times10^{-11}\pm6.8\times10^{-12}$	G059.7831+00.0648	19:43:11.28	+23:44:04.9	8.6	1.0	0.08	0.743
1FGL J2032.8+3928	308.2003	39.4701	0.2507	2.59±0.07	$5.1\times10^{-11}\pm1.4\times10^{-11}$	G078.4705−00.1830	20:31:53.30	+39:19:36.8	5	< 1.2	0.23	0.908
1FGL J2040.0+4157c	310.0154	41.9533	0.1970	2.66±0.06	$7.9\times10^{-11}\pm1.2\times10^{-11}$	G081.5168+00.1926	20:39:57.79	+41:59:13.9	5	< 1.1	0.04	0.195

Table 1: Positional coincidence of Fermi sources with MYSOs. The *c* in the Fermi source name indicates that based on the region of the sky the source is considered to be potentially confused with Galactic diffuse emission

Actual coincidence	Simulated 1° -bin	Probability 1° -bin	Simulated 2° -bin	Probability 2° -bin
13	3.9± 1.9	2.2×10^{-6}	3.3±1.7	2.0×10^{-8}

Table 2: Statistical results obtained from simulations with a random distribution in galactic longitude.

Actual coincidence	Simulated 20° -bin	Probability 20° -bin	Simulated 40° -bin	Probability 40° -bin
13	5.17± 2.07	1.5×10^{-4}	3.8± 1.9	1.6×10^{-6}

Table 3: Statistical results obtained from simulations constrained both in galactic latitude and galactic longitude. The binning is the one used in galactic longitude.

Results

- We find 13 Fermi sources being positionally coincident with 24 YSOs (see Table 1).

- 8 of these Fermi sources have not any catalogued possible counterpart (like SNR, PWN, pulsar, etc.) to the gamma emission within the error ellipse.

- From Table 2 we can see that there is a correlation at 5σ level.

- The probability of a pure chance association is as low as 2.0×10^{-8} for the 2º-binning simulations (2.2×10^{-6} for the 1º-binning).

When we considered the restrictions in both *l* and *b* (see Table 3), the chance probability raised, but still shows a quite negligible values (10^{-6}) .

One of the most interesting coincidences is the one of the Fermi source **1FGL J1943.4+2340** (see Fig. 3). We can see in the radio map from the NVSS that there is a region of massive star formation with many X-ray sources, where the YSO from the RMS survey is located.

Another interesting case is the one of the Fermi source **1FGL J1853.1+0032** (see Fig. 4). This source has an error circle of more than 0.5º and thus, we find a large number of sources inside the error ellipse. Some of the sources are the SNR G033.7+0.00, SNR G033.6+0.01 and the pulsar PSR J1852+0040 which, even when the source has no proposed counterpart, are probable candidates to be the responsible of the γ-ray emission.

Finally, we can comment the case of the Fermi source **1FGL 1925.0+1720**. There is a likely extended radio source within the error ellipse of the Fermi source, and near the two RMS sources.

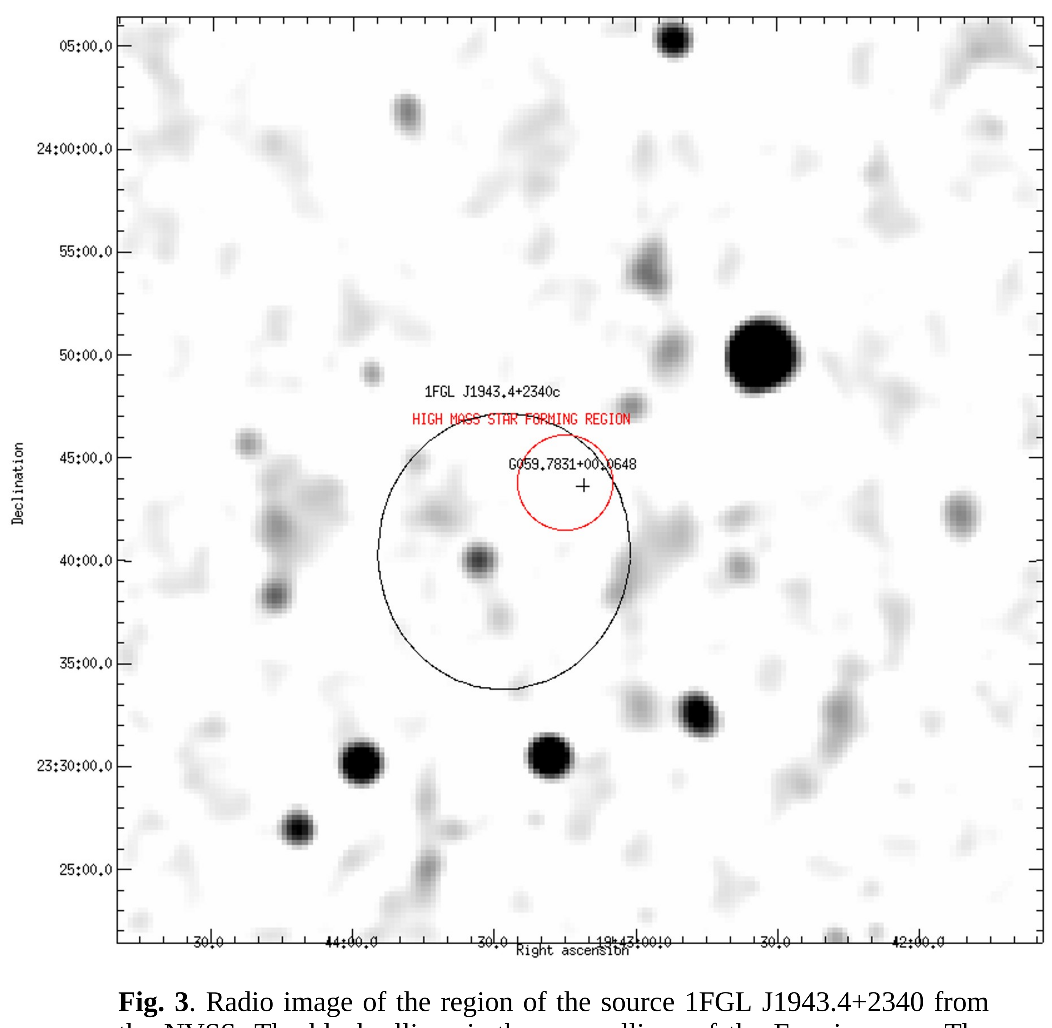

Fig. 3. Radio image of the region of the source 1FGL J1943.4+2340 from the NVSS. The black ellipse is the error ellipse of the Fermi source. The black cross is a YSO from the RMS survey and the red circle is the position of a high mass star forming region. In the last region we find several X-ray sources.

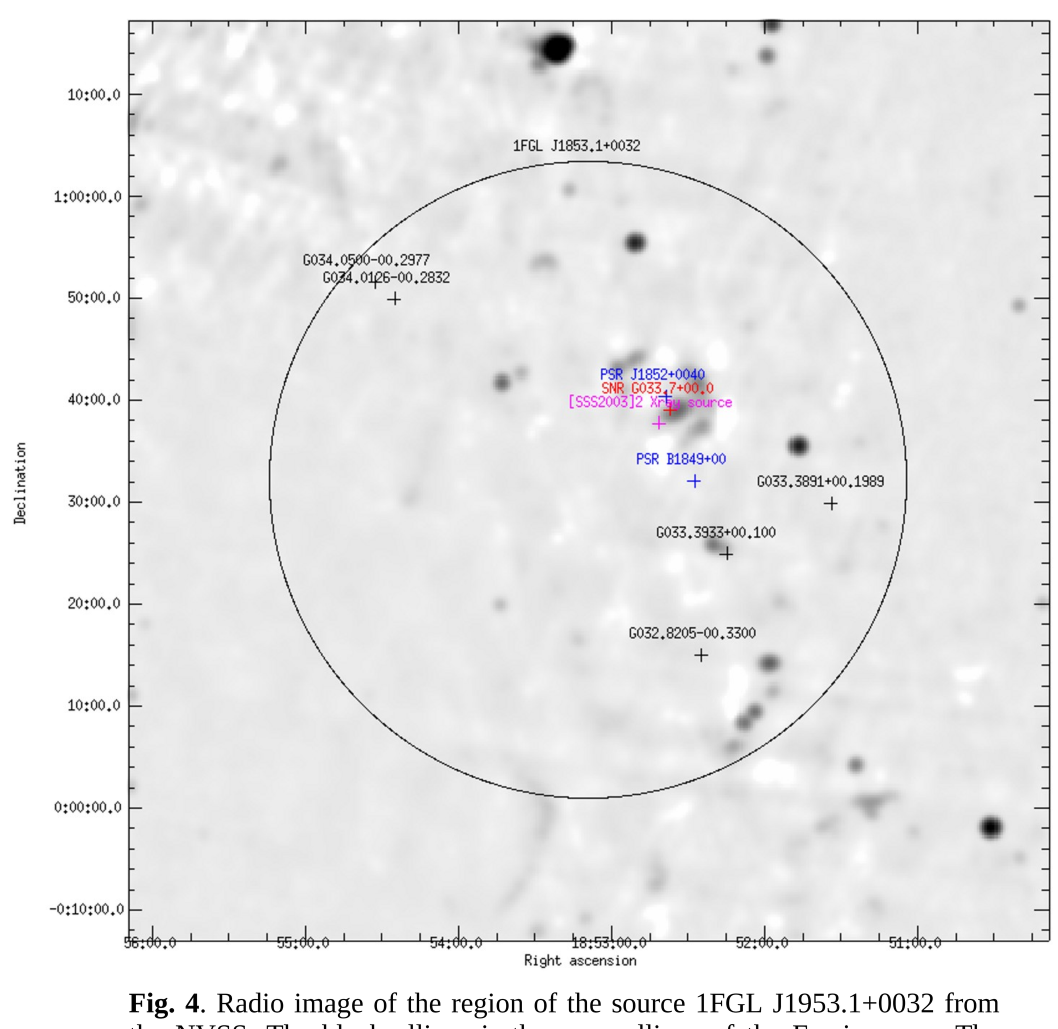

Fig. 4. Radio image of the region of the source 1FGL J1953.1+0032 from the NVSS. The black ellipse is the error ellipse of the Femi source. The black crosses are YSOs. The colored crosses are other sources inside the error ellipse that migh be counterparts of the Fermi source.

References

Abdo A.A. et al., 2010, ApJ Suplement Series, 188, 405-436
Allington-Smith J.R., Perryman M.A.C., Longair M.S. et al., 1982, MNRAS, 201, 331-344
Araudo A.T., Romero G.E., Bosch-Ramon V., and Paredes J.M., 2007, A&A, 476, 1289-1295
Bell A.R., 1978, MNRAS, 182, 147
Bosch-Ramon V., Romero G.E., Araudo A.T. and Paredes J.M., 2010, A&A, 511, A8
Garay G., Brooks K.J., Mardones D., and Norris R.P., 2003, ApJ, 587, 739-747
Lumsden S.L., Horae M.G., Oudmaijer R.D., and Richards D., 2002, MNRAS, 336, 621-636
Molinari S., Brand J., Cesaroni R. et al., 1998, A&A, 336, 339–351
Price S.D., Egan M.P., Carey S.J. et al., 2010, AJ, 121, 2819-2842
Romero G.E., Benaglia P. and Torres D.F., 1999, A&A, 348, 868-876
Sridharan T.K., Beuther H., Schilke P. et al., 2002, ApJ, 566, 931-944
Urquhart J.S., Horae M.G., Purcell C.R. et al. , 2009, 2009, A&A 501, 539-551